ROBUST RETINAL IMAGE REGISTRATION USING EXPECTATION MAXIMISATION WITH MUTUAL INFORMATION

Parminder Singh Reel[†] *Laurence S. Dooley*[†] *K.C.P Wong*[†] *Anko Börner*[⋆]

[†]Department of Communication and Systems, The Open University, Milton Keynes, United Kingdom
[⋆]Optical Sensor Systems, German Aerospace Center (DLR), Berlin, Germany
Email: [†]{*p.s.reel, l.s.dooley, k.c.p.wong*}*@open.ac.uk*, [⋆]*anko.boerner@dlr.de*

ABSTRACT

Retinal images (RI) are widely used to diagnose a variety of eye conditions and diseases such as myopia and diabetic retinopathy. They are inherently characterised by having non-uniform illumination and low-contrast homogeneous regions which represent a unique set of challenges for *retinal image registration* (RIR). This paper investigates using the *expectation maximization for principal component analysis based mutual information* (EMPCA-MI) algorithm in RIR. It combines spatial features with mutual information to efficiently achieve improved registration performance. Experimental results for mono-modal RI datasets verify that EMPCA-MI together with Powell-Brent optimization affords superior robustness in comparison with existing RIR methods, including the *geometrical features method*.

***Index Terms*—** Image registration, principal component analysis, mutual information, expectation-maximization algorithms, retinopathy.

1. INTRODUCTION

Image registration is an integral procedure in many computer vision and image processing applications [1], [2]. For example, registering medical images in conjunction with image fusion facilitates disease diagnosis and treatment planning [3] in many areas of human anatomy. *Retinal images* (RI) of a patient need to be registered in order to diagnose eye conditions and diseases such as myopia, glaucoma and diabetic retinopathy [4]. *Retinal image registration* (RIR) aligns the vessel structures of the retina to assist in ophthalmology, particularly in the tracking and analysis of the advancement of these diseases.

RIR is challenging because the images exhibit spatially non-uniform contrasts and intensity distributions, as well as having large homogeneous non-vascular regions. These collective characteristics can be further compromised by degradations in various pathologies [4]. Existing intensity and feature-based RIR techniques are not always robust to effectively manage RI and have been shown to be dependent on the quality of features extracted, while hybrid approaches which combine intensity and feature techniques are not computationally efficient. This paper investigates the application of a new hybrid-based similarity measure [5], which incorporates RI spatial information with *mutual information* (MI). The corresponding RIR performance is compared with an alternative current feature-based method for a series of mono-modal RI test scenarios and found to be more robust.

The remainder of the paper is organised as follows: Section 2 presents a review of contemporary RIR techniques, while Section 3 details the EMPCA-MI-based RIR framework. Section 4 describes the experimental set-up and analyses the registration performance, with some concluding comments being provided in Section 5.

2. PREVIOUS WORK

RIR can be broadly classified into *feature, intensity* and *hybrid* based techniques [6]. *Feature*-based approaches primarily use extracted vessel structure and landmark points from the RI, while intensity techniques focus solely on pixel intensity information. They can also be combined effectively to form hybrid techniques [1]. Utilising features in RIR is analogous to manual registration, as key structures are extracted from the RI such as optical disk [7], fovea [8] and vascular structural features [9]. An objective function is constructed from the extracted features, which is subsequently optimised to secure the best alignment position of the RI. Dual-bootstrap iterative closest point [10] and its scale-invariant feature transform variants [11], use vascular features of small regions to grow a bootstrap region to accomplish registration. While these methods are computationally efficient, their registration performance is very dependent on the quality of segmentation and degree of overlapping of the extracted features.

The *geometrical features method* (GFM) [12] is a recent feature-based method which has been shown to provide better registration results compared with other existing RIR techniques. By applying *affine moment invariant* (AMI) descriptors, GFM performs closed-boundary region extraction

on vessel segmented RI, before defining a set of control points, which are both rotation and scale invariant, based upon the centre of gravity of each region. Three region pairs are then selected on the basis of their AMI Euclidean distance for use in the registration mapping.

In contrast, *intensity*-based techniques use a *similarity measure* (SM) such as cross correlation, least mean square error, phase correlation or MI [13], [14] to compare and match RI by applying an optimization strategy to maximise the SM within transformation search space. MI has been widely adopted in both mono and multi-modal medical image registration of various parts of the human body. Instead of having pre-processing steps such as segmentation and feature extraction, MI establishes a statistical relationship between the intensity values of the images, though because of the challenging characteristics of RI, MI does not perform very effectively [15].

Hybrid approaches combine various aspects of the aforementioned feature and intensity methods, such as for example, using extracted vascular structures [16] together with spatial information as in regional MI [17] and feature neighbourhood MI [18], [19]. While these techniques use a covariance matrix to reduce data complexity [17] instead of high-dimensional histograms, as the spatial information expands, it does lead to a commensurate increase in computational time. EMPCA-MI [5], [20] is a hybrid-based algorithm used for registering brain computed tomography and magnetic resonance images by combining spatial information with MI. It has been shown to exhibit superior robustness in its registration performance in the presence of non-uniform intensity and noise, and given the innately challenging characteristics of RI this provided the impetus to investigate applying EMPCA-MI [5] within a RIR context.

3. PROPOSED REGISTRATION FRAMEWORK

3.1. Principles of Retinal Image Registration (RIR)

RIR consists of aligning a reference image I_R with a sensed image I_S in a multi-step process [2]: *i)* transforming the coordinates of I_S in a known reference space; *ii)* generating a new interpolated image $I_S^\star$ in the reference space; *iii)* comparing $I_S^\star$ with the reference image I_R using a predefined SM; and *iv)* optimizing transformation μ to achieve the best alignment at μ_{reg}. This can be generalised as a maximisation problem:

$$\mu_{reg} = \arg\max_{\mu} SM(I_R, \mu(I_S)) \tag{1}$$

where μ_{reg} gives the best registration parameter settings. The interpolation method used for transforming I_S plays a central role in RIR, since interpolation artefacts can considerably impact upon SM performance leading to increased registration errors [2].

3.2. EMPCA-MI as a Similarity Measure

EMPCA-MI [5], [20] is a recently introduced SM for image registration that efficiently incorporates spatial information together with MI without incurring high computational overheads. As illustrated in the example in Fig. 1(a), it comprises three steps involving pre-processing (image data rearrangement), EMPCA and MI calculation. Note the block colours in Fig. 1(a) symbolise pixels for pre-processing and not the actual pixel itself. I_R and I_S are both pre-processed (*Step I*) in vector form for a given neighbourhood radius *r*, so the spatial and intensity information is preserved. The first *P* principal components X_R and X_S of the respective reference and sensed images are then iteratively computed by EMPCA in *Step II*, instead of solving the covariance matrix. The final MI value is calculated between X_R and X_S in *Step III*, with a higher MI value meaning the two images are better aligned. In the EMPCA-MI algorithm, only the first principal component is considered, i.e., *P=1* since this is the direction of highest variance and represents the most dominant feature. EMPCA-MI can be formally expressed as:

$$EMPCA{-}MI(I_R, I_S) = \sum_{X_R, X_S} p(X_R, X_S) \log \frac{p(X_R, X_S)}{p(X_R), p(X_S)} \tag{2}$$

where $p(X_R)$ and $p(X_S)$ are the individual probabilities of X_R and X_S respectively, while $p(X_R,X_S)$ is their joint probability.

3.3. Transformation and other registration settings

RI acquisition inherently leads to a distortion between I_S and I_R which can be modelled as a *similarity transformation* [12], [18], [19]. This special form of the global affine transform [21] represents RI distortion as either eye or camera (*x*-*y* translational and rotational θ) motion, with magnification changes due to using different equipment or the motion in the direction of the optical axis being modelled as a uniform scaling *S* [22]. These four parameters can be formulated as:

$$\begin{bmatrix} x' \\ y' \end{bmatrix} = \begin{bmatrix} t_x & S\cos\theta & -S\sin\theta \\ t_y & S\sin\theta & S\cos\theta \end{bmatrix} \begin{bmatrix} 1 \\ x \\ y \end{bmatrix} \tag{3}$$

Where (x, y) and (x', y') are the original and transformed pixel positions respectively. The notation μ (t_x, t_y, θ, S) is adopted to represent the four key registration parameters: the x translation, the y translation, the rotation θ and scaling factor S of transform μ. To automatically determine these parameters, Powell's multidimensional direction set method is applied along with Brent optimization [23] for line minimization, because this provides a local search which is accurate, fast and particularly suited to RIR [2].

4. EXPERIMENTAL SET-UP AND RESULTS

To evaluate the RIR, the clinical dataset DRIVE [24], from a Dutch diabetic retinopathy screening program was used.

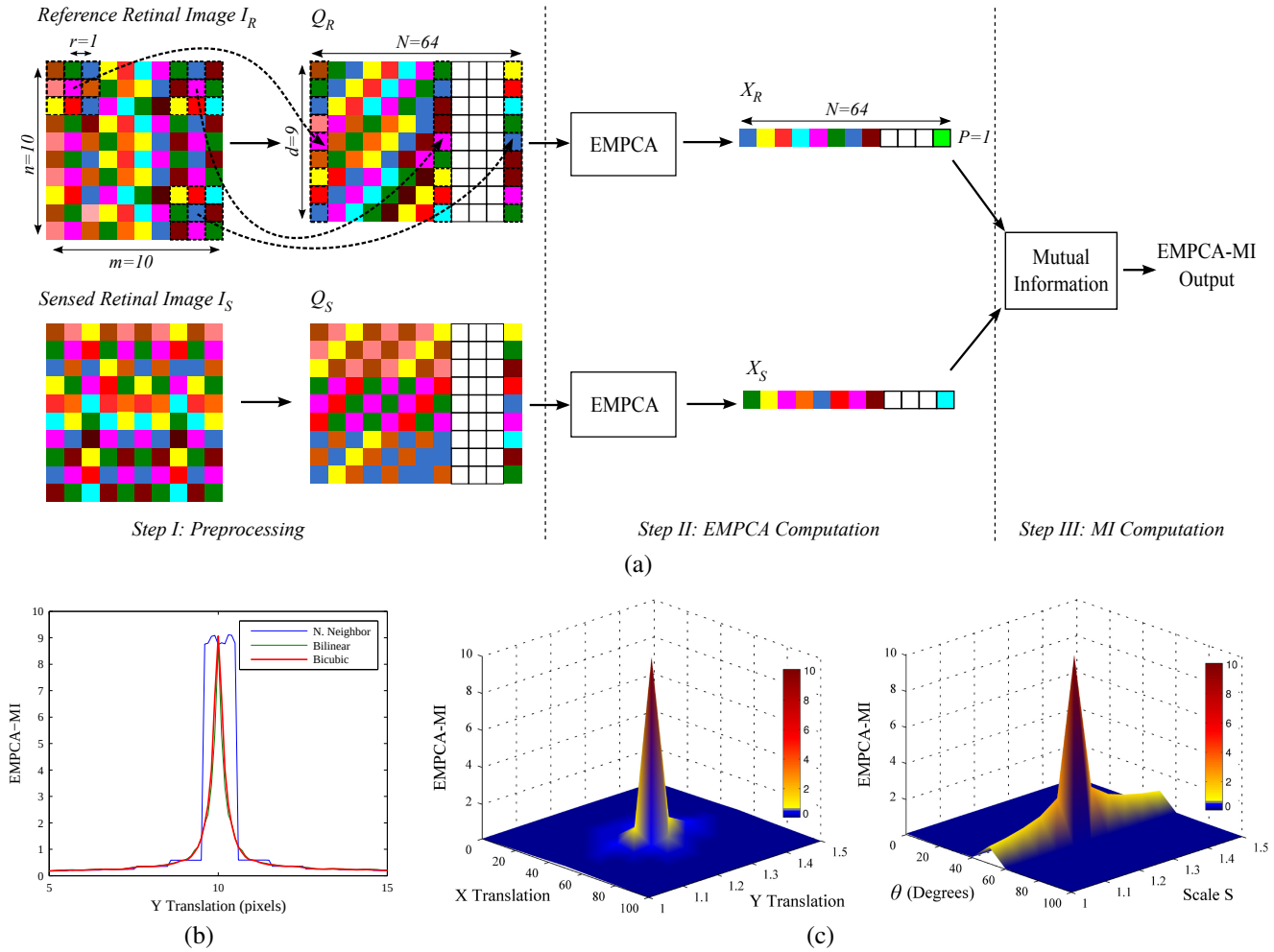

Fig. 1. (a) Example of EMPCA-MI computation using a RI pair of size *10* x *10* pixels (with P=1 and r=1). (b) 2D EMPCA-MI trace of the y translation for different interpolators. (c) EMPCA-MI traces and the corresponding colour bar for Bicubic interpolation.

This comprises twenty colour images with spatial resolution 768 by 584 pixels and 45° circular fields of view. All RI contain non-uniform illumination and low contrast, which accentuates the registration challenge. Since reference images were not available for this database, they were simulated to establish the requisite ground truth, by mis-registering them by a known transformation μ_{grd}, with the original images considered as the sensed images. RIR was undertaken on only the green channel, since this has the highest contrast compared with the red and blue channels, which can often be saturated and contain acquisition noise [12]. For optimization, the tolerance thresholds for the Powell and Brent criteria were set to 10^{-5} and 10^{-3} respectively [2], with the maximum number of iterations being 200. As delineated in Section 2, GFM [12] is one of the leading feature-based solutions, so this was chosen as the comparator in the following RIR experiments.

4.1. Results Discussion

As alluded in Section 3.1, interpolation plays key role in the registration process and can significantly perturb the performance of a SM. Before analysing the performance of EMPCA-MI for RIR, the influence of different interpolation techniques including *nearest neighbour* (NN), Bilinear and Bicubic on EMPCA-MI was examined. Various simulation runs for EMPCA-MI using different *Image Pairs* from the dataset [24] were performed using Bicubic, Bilinear and NN interpolation. It was observed that Bicubic interpolation consistently provided the lowest registration error as evidenced in Fig 1(b), which shows the respective EMPCA-MI traces for *Image Pair 3*, with μ_{grd}*=(0, 10, 0, 1)* for all three interpolators. As both the Bilinear and NN interpolators generated higher errors, the Bicubic interpolator was considered for the various RIR experiments. Fig. 1(c) shows the EMPCA-MI results for *Image Pair 6*, with μ_{grd}*=(6, 6, 50, 1.2)* where all

Image Pair No.	*Scenario 1*		*Scenario 2*		*Scenario 3*		*Scenario 4*
	μ_{grd}=(0, 0, 5°, 1)		μ_{grd}=(0, 0, 60°, 1)		μ_{grd}=(5, 5, 20°, 2.8)		μ_{grd}=(8, 9, 45°, 0.8)
	Δt_x, Δt_y, $\Delta\theta$, ΔS		Δt_x, Δt_y, $\Delta\theta$, ΔS		Δt_x, Δt_y, $\Delta\theta$, ΔS		Δt_x, Δt_y, $\Delta\theta$, ΔS
	GFM [12]	EMPCA-MI *P=1, r=1*	GFM [12]	EMPCA-MI *P=1, r=1*	GFM [12]	EMPCA-MI *P=1, r=1*	EMPCA-MI *P=1, r=1*
1	0, 0, 0.02, 0	0, 0, 0.01, 0	0, 0, 0.01, 0	0, 0, 0.01, 0	0, 0, 0.038, 0.001	0, 0, 0.021, 0.001	0, 0, 0.054, 0.001
2	0, 0, 0.05, 0	0, 0, 0.03, 0	0, 0, 0.01, 0	0, 0, 0.01, 0	0, 0, 0.026, 0.002	0, 0, 0.073, 0.000	0, 0, 0.137, 0.008
3	0, 0, 0.62, 0	0, 0, 0.60, 0	0, 0, 0.02, 0	0, 0, 0.16, 0	0, 0, 1.227, 0.000	0, 0, 1.425, 0.021	0, 0, 2.268, 0.013
4	0, 0, 0.02, 0	0, 0, 0.01, 0	0, 0, 0.09, 0	0, 0, 0.06, 0	0, 0, 0.052, 0.005	0, 0, 0.021, 0.001	0, 0, 0.057, 0.006
5	0, 0, 0.10, 0	0, 0, 0.08, 0	0, 0, 0.17, 0	0, 0, 0.08, 0	**0, 0, 0.138, 0.075**	**0, 0, 0.102, 0.013**	0, 0, 0.037, 0.006
6	0, 0, 0.00, 0	0, 0, 0.00, 0	0, 0, 0.00, 0	0, 0, 0.01, 0	0, 0, 0.170, 0.002	0, 0, 0.091, 0.006	0, 0, 0.027, 0.002
7	0, 0, 0.05, 0	0, 0, 0.04, 0	0, 0, 0.02, 0	0, 0, 0.01, 0	0, 0, 0.045, 0.013	0, 0, 0.079, 0.009	0, 0, 0.124, 0.005
8	0, 0, 0.11, 0	0, 0, 0.08, 0	0, 0, 0.12, 0	0, 0, 0.11, 0	0, 0, 0.070, 0.003	0, 0, 0.063, 0.006	0, 0, 0.177, 0.009
9	-	0, 0, 0.05, 0	-	0, 0, 0.15, 0	-	0, 0, 0.158, 0.010	0, 0, 0.054, 0.003
10	0, 0, 0.02, 0	0, 0, 0.01, 0	0, 0, 0.04, 0	0, 0, 0.03, 0	0, 0, 0.006, 0.010	0, 0, 0.002, 0.003	0, 0, 0.146, 0.001

Table 1. Registration errors for four scenarios of retinal image pairs. μ_{grd} is ground truth transform and Δt_x, Δt_y, $\Delta\theta$, ΔS are registration errors for the similarity transformation.

four parameters of the similarity transformation are used for mis-registration. This highlights the smooth convergence of EMPCA-MI to a single solution verifying the appropriateness of applying Powell-Brent optimisation to the challenge of RIR.

Table I displays the comparative registration results for four different scenarios of ten *Image Pairs* for both GFM and EMPCA-MI. In *Scenarios 1* and *2* only one registration parameter varies i.e., rotation θ=5° and θ=60° with the other parameters being fixed, while in *Scenarios 3* and *4*, all four registration parameters vary, including *S* to reflect the RI which have been acquired using different equipment magnifications. Transform parameter settings for the first three scenarios were chosen as in [12], to enable a direct comparison between the performance of EMPCA-MI and GFM. For example, the *Image Pair 5* registration error in *Scenario 3* for GFM and EMPCA-MI is respectively (*0, 0, 0.138, 0.075*) and (*0, 0, 0.102, 0.013*) for the Δt_x, Δt_y, $\Delta\theta$, ΔS parameters. This reveals that EMPCA-MI afforded superior and more robust registration performance compared to GFM in variable contrast and illumination conditions. While only 10 of the 20 *Image Pairs* are displayed in Table 1, the recurring observation regarding the robust RIR performance of EMPCA-MI applies also to the other 10 pairs, which were all correctly registered. It is especially notable to highlight that EMPCA-MI successfully registered *Image Pair 9*, whereas GFM failed to converge to a RIR. The reason for this is that the closed boundary regions extracted from *Image Pair 9* have similar shapes and their corresponding AMI are very close to each other, so GFM was unable to register them successfully. In contrast, as EMPCA-MI does not rely on feature extraction, but on spatial features and MI, it is more robust in being able to register this test *Image Pair*.

Fig. 2 shows an example of the qualitative RIR results of *Image Pair 9* for *Scenario 4*, using checkerboard overlaying method [2], with I_R and I_S in light and dark gray respectively. The continuity of the vessel structures is palpable to validate that EMPCA-MI has effectively registered the RI.

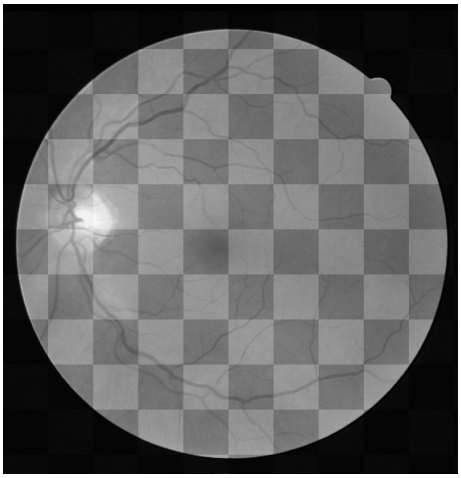

Fig. 2. Checkerboard overlay [2] illustration of *Image Pair 9*.

5. CONCLUSION

This paper has applied a new similarity measure using *Expectation Maximization for Principal Component Analysis with Mutual Information* (EMPCA-MI) to successfully achieve retinal image registration (RIR). Retinal images are especially challenging because of their inherent characteristics of low contrast, non-uniform illumination and large number of homogeneous regions. Quantitative results for mono-modal clinical datasets confirm EMPCA-MI consistently outperformed the *geometric features method* in terms of RIR robustness, while concomitantly providing analogous registration accuracy.

6. REFERENCES

[1] J. B. A. Maintz and M. A. Viergever, "A survey of medical image registration," *Medical Image Analysis*, vol. 2, no. 1, pp. 1–36, Mar. 1998.

[2] B. Zitová and J. Flusser, "Image registration methods: a survey," *Image Vision Comput.*, vol. 21, no. 11, pp. 977–1000, Oct. 2003.

[3] D. L. G. Hill, P. G. Batchelor, M. Holden, and D. J. Hawkes, "Medical image registration," *Phys. Med. Biol.*, vol. 46, no. 3, pp. R1–R45, Mar. 2001.

[4] C. Sanchez-Galeana, C. Bowd, E. Z. Blumenthal, P. A. Gokhale, L. M. Zangwill, and R. N. Weinreb, "Using optical imaging summary data to detect glaucoma," *Ophthalmology*, vol. 108, no. 10, pp. 1812–1818, Oct. 2001.

[5] P. S. Reel, L. S. Dooley, and K. C. P. Wong, "Efficient image registration using fast principal component analysis," in *(ICIP 2012)*, 2012, pp. 1661–1664.

[6] F. Laliberte, L. Gagnon, and Y. Sheng, "Registration and fusion of retinal images-an evaluation study," *IEEE Trans. Med. Imag.*, vol. 22, no. 5, pp. 661 –673, May 2003.

[7] J. Xu, O. Chutatape, E. Sung, C. Zheng, and P. Chew Tec Kuan, "Optic disk feature extraction via modified deformable model technique for glaucoma analysis," *Pattern Recogn.*, vol. 40, no. 7, pp. 2063–2076, July 2007.

[8] H. Li and O. Chutatape, "Automated feature extraction in color retinal images by a model based approach," *IEEE Trans. Biomed. Eng.*, vol. 51, no. 2, pp. 246 –254, Feb. 2004.

[9] M. Sofka and C.V. Stewart, "Retinal vessel centerline extraction using multiscale matched filters, confidence and edge measures," *IEEE Trans. Med. Imag.*, vol. 25, no. 12, pp. 1531 –1546, Dec. 2006.

[10] C.V. Stewart, C.-L. Tsai, and B. Roysam, "The dual-bootstrap iterative closest point algorithm with application to retinal image registration," *IEEE Trans. Med. Imag.*, vol. 22, no. 11, pp. 1379 –1394, Nov. 2003.

[11] C.-L. Tsai, C.-Y. Li, G. Yang, and K.-S. Lin, "The edge-driven dual-bootstrap iterative closest point algorithm for registration of multimodal fluorescein angiogram sequence," *IEEE Trans. Med. Imag.*, vol. 29, no. 3, pp. 636 –649, Mar. 2010.

[12] S. Gharabaghi, S. Daneshvar, and M. Sedaaghi, "Retinal image registration using geometrical features," *J. Digit. Imaging*, pp. 1–11, 2012.

[13] F. Maes, A. Collignon, D. Vandermeulen, G. Marchal, and P. Suetens, "Multimodality image registration by maximization of mutual information," *IEEE Trans. Med. Imag.*, vol. 16, no. 2, pp. 187 –198, Apr. 1997.

[14] M. Skokan, A. Skoupy, and J. Jan, "Registration of multimodal images of retina," in *(EMBS/BMES 2002)*, 2002, vol. 2, pp. 1094 – 1096.

[15] L. Kubecka and J. Jan, "Registration of bimodal retinal images - improving modifications," in *26th Annual International Conference of the IEEE Engineering in Medicine and Biology Society, 2004. IEMBS '04*, Sept. 2004, vol. 1, pp. 1695 –1698.

[16] T. Chanwimaluang, G. Fan, and S.R. Fransen, "Hybrid retinal image registration," *IEEE Trans. Inf. Technol. Biomed.*, vol. 10, no. 1, pp. 129 –142, Jan. 2006.

[17] D. B. Russakoff, C. Tomasi, T. Rohlfing, and C. R. Maurer, "Image similarity using mutual information of regions," in *(ECCV 2004)*, vol. 3023, pp. 596–607. 2004.

[18] P. A. Legg, P. L. Rosin, D. Marshall, and J. E. Morgan, "Incorporating neighbourhood feature derivatives with mutual information to improve accuracy of multi-modal image registration.," in *MIUA*, 2008, pp. 39–43.

[19] P. A. Legg, P. L. Rosin, D. Marshall, and J. E. Morgan, "A robust solution to multi-modal image registration by combining mutual information with multi-scale derivatives," in *(MICCAI 2009)*, number 5761, pp. 616–623. Jan. 2009.

[20] P. S. Reel, L. S. Dooley, and K. C. P. Wong, "A new mutual information based similarity measure for medical image registration," in *(IET IPR 2012)*, July 2012, pp. 1 –6.

[21] L. G. Brown, "A survey of image registration techniques," *ACM Comput. Surv.*, vol. 24, no. 4, pp. 325–376, Dec. 1992.

[22] N. Ryan, C. Heneghan, and P. de Chazal, "Registration of digital retinal images using landmark correspondence by expectation maximization," *Image Vision Comput.*, vol. 22, no. 11, pp. 883–898, Sept. 2004.

[23] W. H. Press, S. A. Teukolsky, W. T. Vetterling, and B. P. Flannery, *Numerical Recipes 3rd Edition: The Art of Scientific Computing*, Cambridge University Press, 3 edition, Sept. 2007.

[24] J. Staal, M.D. Abramoff, M. Niemeijer, M.A. Viergever, and B. van Ginneken, "Ridge-based vessel segmentation in color images of the retina," *IEEE Trans. Med. Imag.*, vol. 23, no. 4, pp. 501 –509, Apr. 2004.